An Ultrasonic Technique to Monitor Fatigue Damage in Aircraft Structures

S. ZIRINSKY*
Harry Belock Associates, Great Neck, N.Y.

A procedure is proposed for the development of a practical and reliable nondestructive technique toward the in situ monitoring within aircraft structures of fatigue damage, prior to and during propagation of running fatigue cracks. The technique utilizes precalibrated ultrasonic surface wave signal strength changes and can monitor both areas of uniform stress and points of stress concentration. Multiple sensor installations can be effectively monitored by a single portable instrument obtaining both manual readout and permanent oscillograph records, easily interpretable. The procedure is applicable to either continuous in-flight readout or intermittent readout during periodic ground maintenance checkouts. The requirements for establishing calibration data for both laboratory and field testing are presented along with a discussion of limitations in the technique. A proposed basis for interpretation of the ultrasonic data using a simple analytical cumulative damage model also is presented.

Nomenclature

H = ultrasonic signal pulse height displayed on the oscilloscope or oscillograph pen displacement
A = volumetric fatigue zone at a uniform stress level
B = stress concentration zone adjacent to the starting notch and fatigue crack
D = ultrasonic energy loss arising from fatigue damage
v = volume of stress-dependent fatigue-damage zone
w = ultrasonic beam width and transducer width
K_e = electromechanical conversion constant which includes the transducer efficiency and electrical circuit losses
l = length of stress-dependent fatigue-damage zone
s = surface area of stress-dependent fatigue-damage zone
x = length of stable fatigue crack
n_i = number of fatigue cycles
n_{ci} = number of fatigue cycles to crack initiation
n_{xi} = number of fatigue cycles during fatigue-crack propagation
a = slope of log-log plot of fatigue-damage index vs number of fatigue cycles
Y = fatigue-damage index
N = number of cycles for $Y = 1$
M = number of cycles to failure
L_p = ultrasonic energy loss at the transducer-specimen surface interface
L_r = ultrasonic energy loss within volume traversed by ultrasonic beam
L_s = ultrasonic energy loss due to surface factors such as films, surface roughness, etc.
L_c = ultrasonic energy loss arising from scattering of the signal transmission at the crack after the crack partially traverses the width of the signal zone
z = total number of flights prior to start of monitoring
j = 1, 2, . . . , m number of flights monitored
H_j = a reference ultrasonic pulse amplitude arbitrarily established when the probe is situated within a low-stress region adjacent to the test area of interest; the electrical settings are locked; H_j can be established after z flights; all subsequent measurements use the same probe configuration and the same electrical settings
$\sum_{i=0}^{m} Y(n_j + z)$ = value of fatigue-damage index after z plus m flights
Y_{cr} = critical fatigue damage obtained at fatigue-crack initiation
N_{cr} = total number of flights up to fatigue-crack initiation
$\bar{a}$ = average exponent with repetitive block spectrum loading for fatigue-damage index vs number of flights

Presented as Paper 67-793 at the AIAA 4th Annual Meeting, Anaheim, Calif., October 23–27, 1967; submitted November 15, 1967; revision received March 1, 1968.

* Materials Consultant, Structures and Materials Division.

I. Introduction

ACCURATE forecasts of the fatigue-limited life of a critical structural component within an aircraft are contingent upon a number of indirect factors which depend principally upon the correlation between predicted design life and accumulated service history. These fatigue-service life forecasts would follow design predictions where effective quality control during manufacture and service installation is observed. In practice, however, these factors do not always apply as is evidenced by the *FAA Airworthiness Bulletins* reporting a high frequency of fatigue-induced cracks causing extensive repair work to maintain airworthiness.

It can be noted that the airworthiness standards ("Transport Category Airplanes"—Pt. 25 of the *Federal Aviation Regulations*) specifies a margin of safety of 1.5 for static structural load requirements. This can be translated in well-defined structural design requirements even with the presence of stress concentrations. Substantiating load tests are considered necessary only where structural analysis has not been proven by previous reliable experience. Reliable design criteria for static loading can be readily established from the available materials data published in *MIL-HDBK-5*. On the other hand, specific margins of safety for fatigue-limited design criteria are not as clearly defined as with static loading. This difference is due to the much greater variation observed for fatigue properties as influenced by stress concentrations arising from surface markings and alloy inhomogeneities, plus other service factors such as fretting and corrosion.

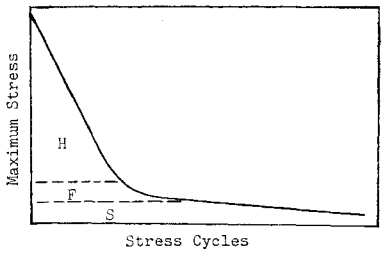

Fig. 1 Characteristic microstructural fatigue damage regions for S/N curve.

Design techniques relating complex loading spectra to the fatigue properties obtained by established laboratory test procedures, are still the subject of considerable controversy and continued study. Therefore the airworthiness standards for fatigue-limited design criteria establish requirements closely relating the fatigue-limited structural performance to the specific aircraft-loading spectrum as established by prior performance history or by tests, or both. The most specific design criterion to be met is a blanket specification necessitating the use of design procedures that will not result in catastrophic failure of the airplane where fatigue failures of specified structural components are obtained. This generally calls for margins of safety exceeding those used for static loading service limits. The major reason for this involves the lack of understanding of the stress-strain relationships under fatigue-type loading. Therefore the prediction of strain-limiting failure can not be readily made for fatigue, as can be done for static loading.

The present state-of-the-art for the analysis of microstructural aspects of fatigue[1] clearly indicates that a well-established strain configuration develops that eventually leads to macrocracks. The distribution of microcracks just prior to unstable macrocrack initiation and propagation, varies with the metallurgical type and state of material, surface condition, and type of fatigue loading. These microcrack distributions cannot be correlated with normal strain-measuring techniques. Many studies have shown, though, that unique microstrain (slip band distributions) and microcrack distributions are obtained under different fatigue-failure conditions.

For example, Wood,[2] a leading worker in this field, has described the microstructural processes associated with accumulated fatigue damage as a function of stress level. He has divided the standard *S-N* curve into three convenient parts (see Fig. 1).

1) The *H* region. This is the high stress-short life region and covers the section of the *S-N* curve where the fatigue life is highly sensitive to stress level. This region is characterized by distinctive microstructural changes within the metal grains. Characteristic submicroscopic defects increase in density up to 5% of the fatigue life. From 5 to 99% of the fatigue life, the defects grow into microcracks and cluster strongly at the metal grain boundaries. Just prior to fatigue failure, a localized coalescence of the microcracks develops into a macrocrack.

2) The *F* region. This region starts below the knee of the *S-N* curve and proceeds over a significant portion of the cyclic life. The negative slope of the stress vs cyclic life curve is much smaller than that observed for the *H* region. In addition, a considerable scatter band is observed for a particular fatigue test series which is influenced principally by the initiation of macrocracks. The microstructural changes that occur within this region differ somewhat from those observed in the *H* region. Strain hardening occurs in both the *H* and the *F* region.

3) The *S* region. This region is actually an extension of the *F* region and is characterized by the development of slip markings, but no regions of fatigue damage. Specimen failures are not generally observed within this region regardless of the number of cycles.

4) Cumulative damage. This factor cannot generally be estimated in a simple manner, i.e., the rate of fatigue-damage generation is not a simple function of prior accumulated damage. Wood[2] has shown that, for "soft" metals and alloys, *H* amplitude precycling causes the *H* mechanism to extend into the *F* region, while F amplitude precycling accelerates the damage developed in the *H* region. Studies by other investigators[3] with "hard" metals indicate that extension of fatigue life by preunderstressing ("coaxing") below the fatigue limit is not applicable for all types of structural alloys since the effect is found with steels but not with 7075-T6 aluminum. In addition, combined stresses will generally accelerate specimen failure beyond that observed for the case of the mean stress being zero. These factors generally complicate the development of theoretical, statistical fatigue-damage models that rely upon simplifying assumptions for the development of fatigue damage within complex loading environments such as are obtained with airplane structural members. The preceding discussion illustrates the need for a direct technique to quantitatively assess the development of fatigue damage within a structural component.

Other basic materials studies utilizing internal friction analysis techniques[4] have indicated that high-frequency ultrasonic waves are readily attenuated by the presence of microstrains and microcracks. Since the industrial use of ultrasonic techniques is well established for the detection of macrocracks, it would appear that the ultrasonic techniques may be applicable toward the nondestructive measurement of fatigue strain prior to macrocrack formation.

Based upon these considerations, the writer conducted an experimental program to explore the possibilities inherent in this procedure. Practical test procedures were developed yielding highly promising experimental data that allowed for the formulation of a fatigue-damage accumulation concept relating to practical fatigue design and nondestructive monitoring procedures applicable to aircraft maintenance. The preliminary results of this study were presented recently at the 1966 Reliability Symposium and published in their proceedings.

II. Laboratory Studies

The previous discussions clearly illustrate the need for direct techniques[6–11] to quantitatively assess the development of fatigue damage. In spite of the advanced development of ultrasonic techniques, somewhat mixed results have been achieved covering the range of sensitivity of detection.[12] Brosius[12] was not able to detect fatigue damage, prior to the formation of stable fatigue cracks, using $2MH_z$ Rayleigh waves. Fatigue damage in soft aluminum alloys was readily detected with high-frequency dilatational waves (2–10 MH_z).[13] Other studies with MH_z Rayleigh waves

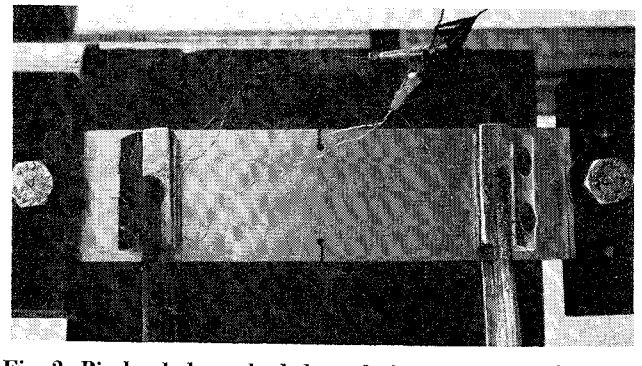

Fig. 2 Pin loaded notched sheet fatigue specimen (tension loading); note, the double transducer probe arrangement clamped to the specimen just below the grips; each probe contains two ½-in. X cut quartz transducers.

required 30% of the fatigue life to be expended prior to the detection of fatigue microcracks.[14] The writer has explored the frequency range of 500 KH_z to 30 MH_z with both dilatational and surface waves (Rayleigh and Lamb waves) for aluminum. It was observed that, for the hard alloys, dilatational waves appeared insensitive to accumulated fatigue damage. When surface waves within the range of 5–10 MH_z were used (Rayleigh waves for bar stock and Lamb waves for sheet stock), the accumulation of fatigue damage in both tension-tension and bending loading was readily and reproducibly detected for both smooth and notched specimens. Materials studied included Al 2024-T3, Al 7075-T6, and others. Only the studies for the aluminum alloys are discussed in this paper.

The ultrasonic studies during fatigue have utilized both pulses-echo and pulse-transmission techniques. Since the laboratory test work involved studies with sheet specimens, angled probes developing Lamb waves were utilized. For heavy section parts similar probes would be utilized to develop Rayleigh waves.

The equipment for tension-tension studies included a 5000-lb Krouse tension-compression fatigue machine, a Sperry Ultrasonic Attenuation Comparator (Style 56A001) plus broadband receiver, and a Sanborn 150 Recorder coupled with auxiliary circuits for readout of a single preselected pulse. The test arrangement is shown in Figs. 2 and 3. The ultrasonic beam is propagated through the gage area between two mounted ultrasonic probes. The signal is displayed at the center of the scope. The variation in height of the pulse is considered to be directly proportional to the attenuation of the ultrasonic pulse height, during the fatigue cycling. The pulse height is recorded automatically on two channels simultaneously. The first is scaled to cover the full pulse-height variation over the channel, and the second is an adjustable expanded scale (10 to 50% of the attenuation of the starting pulse height). The expanded scale is useful in picking up small changes in the attenuation, not observable visually on the oscilloscope. For example, during the fatiguing of notched specimens, the expanded scale indicates a pause in the slope of the oscillograph trace when the stable fatigue crack "pop in" occurs at the notch. A variety of tests were performed to insure that the attenuation observed during the fatigue cycling can be unambiguously related to the microstructural changes occurring during the fatigue exposure. An additional bending fatigue setup was evaluated as shown in Fig. 4. Specimens were evaluated using completely reversed bending with transducers on both sides of the sheet specimen. The loaded part of the specimen was designed with dog-ear mounts to provide a clear edge reflection for the sonic pulses.

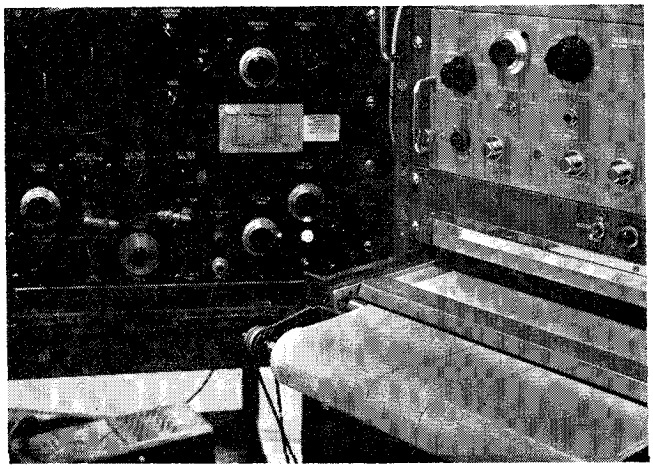

Fig. 3 Ultrasonic pulse display plus oscillograph recording (100% displacement of right trace corresponds to full decay of central peak; left trace is 10_x expansion of right trace at 0 to 10% loss range).

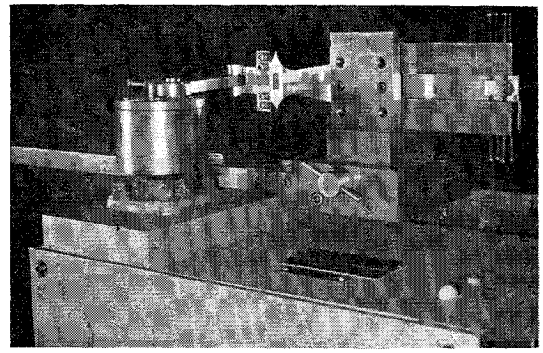

Fig. 4 Reverse bending sheet specimen, constant-stress cross section (grips configured for free sonic path, transducer mounted on free end).

The cumulative damage is predicated upon the development of irreversible strain during loading above the fatigue limit over the entire loading history. The strain is geometrically distributed in accordance with the boundary conditions established by the particular loading geometry and stress concentrations existing at notches. A direct relationship between the ultrasonic attenuation and developing strains (precrack strains and the plastic region leading the running crack) may be obtained by separating out the specific contributions to the over-all ultrasonic attenuation. The specific contributions to the over-all ultrasonic attenuation during the sensing of a notched specimen can be described as follows (refer to Fig. 5).

For the prefatigue crack formulation period, the ultrasonic sensing zone is a rectangular cross section prismatic volume (ignoring slight beam spread) delineated by the dotted lines between the transducers and the two surfaces. Section A is the low elastic strain zone removed from the notched area, and Sec. B is the elliptical high elastic and plastic strain zone developed locally between the notches.

With the ultrasonic sensing volume established to just graze the edge of the notch, prior to macrocrack formation, the attenuation contribution consist of 1) the losses per unit volume in the low elastic strain region (D_A); and 2) the losses per unit volume in the plastic strain or damage region between the notches (D_B).

The measurements of the ultrasonic signal strength is displayed on the oscilloscope and recorded on the attached oscillograph (see Fig. 3). The signal pulse height is inversely proportional to energy losses at the transducer-specimen interface and attenuation losses within the specimen.

At the start of the fatigue test,

$$H_o = 1/[K_o\{L_p + 2l_A(L_v + L_s)w\}]$$

For specimen without stress concentration notches,

$$H_{ni} = 1/[K_o\{L_p + 2l_A(L_v + L_s + D_{A_{ni}})w\}]$$

Normalize the signal change during fatigue loading so as to eliminate the necessity to determine the geometric con-

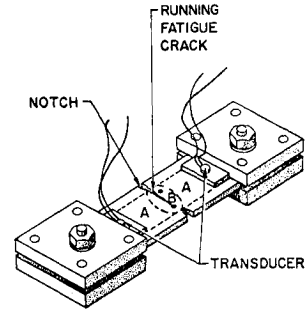

Fig. 5 Sonic path arrangement with notched tensile specimen.

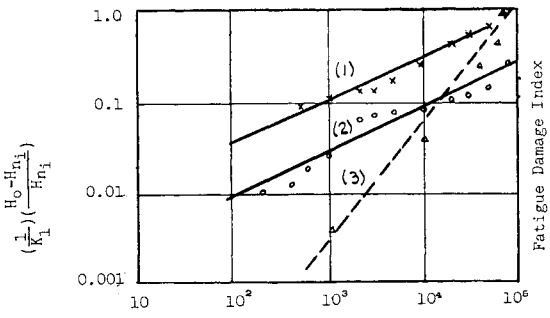

Fig. 6 Fatigue damage for unnotched specimens. Stress cycles: (1) Al 7075-T6, R = 12,000/60,000 psi to 54,000 cycles; (2) Al 2024-T3, R = 8000/40,000 psi to 100,000 cycles; (3) Al 7075-T6, R = 15,000/−15,000 psi to 122,000 cycles.

stants. This is accomplished by taking the difference of the inverse of the signal amplitudes:

$$(1/H_{ni}) - (1/H_o) = K_o \cdot w \cdot 2l_A \cdot D_{A_{ni}}$$

or

$$(H_o - H_{ni})/H_{ni} = K_1(D_{A_{ni}}) \quad (1)$$

For specimens with stress concentration notches (Fig. 5),

$$H_{ni(nc_i<ni<0)} = 1/(K_o\{L_p + [2l_A(L_v + L_s + D_{A_{ni}}) + D_{B_{ni}}]w\})$$

and

$$[(1/H_{ni}) - (1/H_o)]_{(nc_i<ni<0)} = K_o \cdot w[D_{B_{ni}} + 2l_A \cdot D_{A_{ni}}]$$

or

$$[(H_o - H_{ni})/H_{ni}]_{(nc_i<ni<0)} = K_2[D_{B_{ni}} + 2l_A \cdot D_{A_{ni}}] \quad (2)$$

After the initiation of a fatigue crack,

$$H_{ni(nx_i<ni<nc_i)} = \frac{1}{K_o\{L_p + [2l_A(L_v + L_s + D_{A_{ni}}) + D_{B_{ni}} + L_c(x/w)]w\}}$$

and

$$[(1/H_{ni}) - (1/H_o)]_{(nx_i<ni<nc_i)} = K_o \cdot w[D_{B_{ni}} + Lx(x/w) + 2l_A \cdot D_{A_{ni}}]$$

or

$$[(H_{nc_i} - H_{nx_i})/H_{nx_i}]_{(nx_i<ni<nc_i)} = K_2[D_{B_{ni}} + L_c(x/w) + 2l_A \cdot D_{A_{ni}}] \quad (3)$$

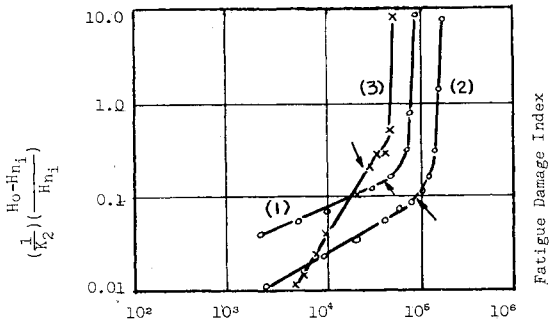

Fig. 7 Fatigue damage for notched specimens. Stress cycles: (1) Al 2024-T3, R = 3000/15,000 psi to 8800 cycles = 2500/12,500 psi to 146,500 cycles; (2) Al 2024-T3, R = 3000/15,000 psi to 42,000 cycles = 2500/12,500 ps to 42,000 cycles; (3) Al 7075-T6, R = 2000/15,000 psi to 25,800 cycles = 2500/12,500 psi to 49,400 cycles.

If it is assumed that D_{Anc_i} and D_{Bnc_i} do not vary after initiation of the fatigue crack, then a simpler relation can be established to evaluate the influence of fatigue-crack propagation, upon the change in ultrasonic signal amplitude:

$$(1/H_{nx_i}) - (1/H_{nc_i}) = K_o \cdot w \cdot L_c(x/w)$$

or

$$(H_{nc_i} - H_{nx_i})/H_{nx_i} = K_3 \cdot L_c \cdot x \quad (4)$$

The data for both smooth and notched specimens loaded in tension-tension for two aluminum alloys, AL 2024-T3 and AL 7075-T6, are plotted in Figs. 6 and 7. For the notched specimens, optical crack length measurements were carried out simultaneously, with the ultrasonic measurements. The results for two of the specimens are shown in Fig. 8. The result for one of the smooth specimens loaded in completely reversed bending is shown in Fig. 6.

An examination of the plots in Figs. 6 and 7 would appear to indicate that, to a rough approximation, the material behavior, prior to fatigue-crack formation, conforms most closely to a linear damage relationship of the following form:

$$Y_{ni} = (n_i/N)^a \quad (5a)$$

Reference 5 discusses the application of this relation to fatigue-damage accumulation as a function of stress dependence and history of spectrum loading. It was also shown that the fatigue damage at either failure, or fatigue-crack initiation, is given by the same relation in which the critical constants are determined as

$$Y_{n_{cr}} = (n_{cr}/N)^a \quad (5b)$$

If it is assumed that Y_{ni} is directly related to D_{ni}, then the results shown in Fig. 6 would indicate that the ultrasonically monitored fatigue-damage accumulation conforms most closely to Eq. (1). This appears to be shown also for the data shown in Fig. 7 prior to fatigue-crack formation. This would also indicate that the fatigue damage within the notch zone does not contribute significantly to the total ultrasonic pulse height change measurement. The large change in signal pulse amplitude within the n_{ni} cycling range (Fig. 7) results from the influence of the L_C contribution for Eq. (4). Figure 8 also shows that a simple relationship between the ultrasonic pulse amplitude variation vs crack growth is not indicated. Further work in this area is required.

III. Application

The experimental results presented in Figs. 6 and 7 appear to correlate well with a linear cumulative damage model. Such a model would then provide an indirect means toward monitoring the development of irreversible fatigue strain, when loading above the fatigue limit. Additional data (not presented) indicate no change in the attenuation of the ultrasonic surface wave when loading below the fatigue limit (unnotched specimens). This observation correlates with

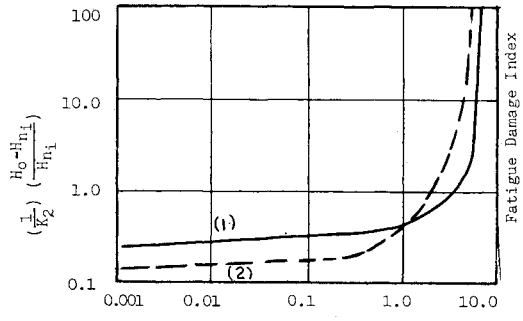

Fig. 8 Ultrasonic monitoring of crack propagation. Crack length (mm): (1) Al 2024-T3 (K_T = 3.7); (2) Al 7075-T6 (K_T = 3.7).

microscopic studies of the S region with the development of slip markings but with no significant microstrain zones. It would therefore be expected that a comprehensive laboratory survey of specimens of varying degree of structural complexity could provide basic calibration data directly applicable to the monitoring of critical points on aircraft structures and thereby provide a means for nondestructive prediction of useful fatigue life. A more comprehensive study would evaluate the stress level, stress ratio, and stress concentration upon the variation of Y_{cr} with N_{cr}.

A number of advantages accrue from the use of the proposed procedure:

1) The ultrasonic technique employs a direct data readout utilizing the variation in the oscilloscope tube pulse height display as a function of developing fatigue damage. Continuous readout is also provided in the form of a simple pen displacement on an oscillograph chart to permit a permanent record. The use of a precalibration procedure can allow for the setting up of a simple procedure for technician control of the instrumentation readings.

2) A one-probe system can service a zone of interest the size of which depends upon the geometry of the test piece. The use of Rayleigh and/or Lamb waves yields a sonic beam of small dispersion providing considerable beam length that can also follow irregular surfaces not containing sharp changes in curvature. Single probes can be used where the beam is directed normal to a sharp edge. A double-probe system is otherwise necessary. The monitoring of a wide area can be readily accomplished with a fixed-probe system by the use of phased arrays employing slow electrical sweeping of the area of interest. Changes in signal attenuation at particular spots within the area swept can be readily picked up and selectively studied.

3) The attenuation of the sonic beam is directly cumulative when traversing several points of interest simultaneously, and is selectively proportional to the degree of strain damage developing at each point. When sonic attenuation indicates the presence of a macrocrack, manual readout on the oscilloscope can identify the point of origin of the macrocrack.

4) Permanently bonded transducer probes provide instrumentation readout for both in-flight continuous monitoring and intermittent ground maintenance scheduled monitoring.

5) The probes are small enough so as to not influence or impair the structural or flight performance of the aircraft.

6) One readout and recording instrumentation package can service all the probes for an installation on an airplane.

7) A manual or automatic alarm level can be utilized based upon the precalibration levels established for the particular area. The procedure is amenable to the development of techniques for continuous electronic sequencing over a number of probe systems feeding the data into an on-line computer preprogrammed with alarm level limits for each probe system. This procedure would provide automatic selection of the first point of incipient failure.

8) The application of this technique can be useful for the eventual development of design guidelines based upon limiting fatigue damage. In addition, the test evaluation costs for advanced designs can be minimized.

The prior laboratory studies have indicated the need for certain precautions in the utilization of this technique. These can be indicated as follows:

1) The electrical settings of the test instrumentation should be locked during a test sequence. Any change in the settings can be readily established and corrected by use of an auxiliary calibration procedure that includes controls of the entire electromechanical circuit and electrical circuits alone. These controls would also monitor any change in transducer efficiency as influenced by the bond between the probe and work piece. The use of a high-quality adhesive bond would minimize any problems in this area.

2) It is necessary for the test operator to exercise caution with regard to observing any change in surface condition within the probed area during the test period since this may cause false indications of changes in signal attenuation. This would include the presence of extraneous layers of oil or water on the surface that can be removed readily.

3) The requirements for probing a particular area must take into account severe geometric discontinuities. For example, the regions adjacent to fasteners can be effectively monitored, but not the fasteners themselves. Intermediate layers of sheet material must be accessible for direct contact with the test probes, but blind areas on these intermediate layers, between the probes, can be monitored.

4) The technique is not highly sensitive to small variations in the rate of accumulation of fatigue damage, but provides dramatic indication of the amounts of fatigue damage that significantly influence the fatigue life of the part. Therefore, when several points contribute to the fatigue-damage indication within a single area being probed, the point most likely to cause failure will dominate the damage display and thereby provide definitive indication of the progress of the failure. If equivalent damage contributions are suspected, they can be selectively analyzed with additional probes without disturbing the starting system.

5) The accuracy of failure prediction of service hardware is contingent upon either a) correlation of field studies with actual environmental service tests to failure, regardless of part complexity, or b) development of laboratory data upon specimens of increasing complexity. In any case, the technique has a "built-in" fail-safe indication whereby the rate of change in attenuation is a function of prior loading history (or developed fatigue damage) which causes the change in ultrasonic signal level to be the greatest as the failure point is approached.

6) All engineering structural alloys are amenable to the use of this technique with the exception of ferritic-type steels and magnetic materials which show deviations in the ultrasonic attenuation fatigue-damage relationship during the early stages. These materials require more careful calibration.

IV. Field Test Evaluation

A proposed procedure can now be presented for field test or service maintenance. An instrumentation assembly is established with a series of miniaturized fixed ultrasonic surface wave probe systems strategically distributed over suspected fatigue zones. A calibrated pulse height is established (and recorded) for each probe system. Periodic measurements of the pulse height are then made and plotted as a function of flight history, established by the number of flights utilizing the concept of the ground-air-ground cycle as the principal fatigue determining factor.[15] The absolute value of the pulse height is not important; only differences arising from stress cycling are important. Where temporary probe-specimen bonds are utilized, the reproducibility, within the test life, from reading to reading (i.e., maintenance cycles), must be established by placing the test probe within a nonfatigued zone adjacent to a calibrating probe and providing the attachment that yields the highest pulse amplitude. The permanently bonded transducers do not require this calibration. When evaluating a structural component that has previously been fatigued, a low stress level test zone is used to determine the arbitrarily established H_o for Eq. (1).

For applying the relations proposed in Sec. II toward field maintenance prediction of service life, Eqs. (1) and (5) can be utilized in the following form:

$$\frac{H_j - H_{(nj+z)}}{H_{(n_i+z)}} = \left(\sum_{j=0}^{m} D_{(nj+z)} \Big/ Kl \right) \tag{6}$$

$$\left(\sum_{j=0}^{m} D(n_j + z) \Big/ D_{cr} \right) = \left(\sum_{j=0}^{m} (n_j + z)^{\bar{\alpha}} \Big/ n_{cr}{}^{\bar{\alpha}} \right) \tag{7}$$

Table 1 Selected experimental values of critical constants for aluminum

Test specimen	α	N	K_1	$\left(\frac{1}{K_{1,2}}\right)\left(\frac{H_o - H_{ni}}{H_{ni}}\right)$
1) Al 7075-T6 unnotched $R = 0.2 = \frac{12{,}000 \text{ psi}}{60{,}000 \text{ psi}}$ $M = 55{,}000$ cycles	0.527	1.2×10^5	1	0.65 (fracture)
2) Al 2024-T3 unnotched $R = 0.2 = \frac{8{,}000 \text{ psi}}{40{,}000 \text{ psi}}$ $M = 99{,}500$ cycles	0.525	1.2×10^6	1	0.27 (fracture)
3) Al 7075-T6 notched ($K_T = 3.7$) $R = 0.2 = \frac{3{,}000 \text{ psi}}{15{,}000 \text{ psi}}$ to 25,800 cycles $R = 0.2 = \frac{2{,}500 \text{ psi}}{12{,}500 \text{ psi}}$ to fracture $M = 49{,}400$ cycles	1.77	7.5×10^4	1	0.165 (crack initiated)
4) Al 2024-T3 notched ($K_T = 3.7$) $R = 0.2 = \frac{3{,}000 \text{ psi}}{15{,}000 \text{ cycles}}$ to 42,000 psi $R = 0.2 = \frac{2{,}500 \text{ psi}}{12{,}500 \text{ psi}}$ to fracture $M = 88{,}500$ cycles	0.51	1.0×10^6	1	0.190 (crack initiated)
5) Al 2024-T3 notched ($K_T = 3.7$) $R = 0.2 = \frac{3{,}000 \text{ psi}}{15{,}000 \text{ psi}}$ to 42,000 cycles $R = 0.2 = \frac{2{,}500 \text{ psi}}{12{,}500 \text{ psi}}$ to fracture $M = 146{,}500$ cycles	0.71	2.1×10^6	1	0.12 (crack initiated)
6) Al 7075-T6 unnotched $R = -1.0 = \frac{15{,}000 \text{ psi}}{-15{,}000 \text{ psi}}$ $M = 122{,}000$ cycles	0.86	5.0×10^4	1	0.92 (fracture)

It would be expected that $\bar{\alpha}$ would be constant with a constant maximum stress and stress ratio. This is demonstrated for several of the cases plotted in Figs. 6 and 7 and summarized in Table 1. The major departure occurs with notched Al 7075-T6 and may be related to the notch susceptibility of the material evaluated. The slope increases with increased stress concentration and alloy notch susceptibility. The higher value for reversed bending can be expected based upon the aspect that complete stress reversal would tend to develop more substructural deformation within the grain structure than when loading in tension-tension only. The comparison of the D_{cr}/K_1 values for the unnotched specimens indicates that in spite of a higher concentration of fatigue damage with reversed bending, the tension-tension loading nucleates the fracture initiating macrocrack more quickly. These results demonstrate the importance of laboratory calibration for the critical constants as a function of material, stress concentration, stress ratio, and maximum stress. There is no change required for testing methods excepting the ability to properly mount and monitor the ultrasonic sensors.

It should be noted that an average value of $\bar{\alpha}$ is used for Eqs. (6) and (7) based upon the initial very simple assumption that the averaging would be statistically valid for repetitive flight histories. The validity of this assumption must be examined when correlating flight-history data with laboratory data. Equations (6) and (7) can be combined to yield a working relationship for field testing:

$$\left[\frac{H_j}{H_{(nj+z)}} - 1\right] K_1 = \frac{D_{cr}}{n_{cr}^{\bar{\alpha}}} \left[\sum_{j=0}^{m} (n_j + z)\right]^{\bar{\alpha}} \quad (8a)$$

or

$$\log\left[\frac{H_j}{H_{(nj+z)}} - 1\right] + \log K_1 = \log D_{cr} + \bar{\alpha}\left[\log\left\{\sum_{j=0}^{m} (n_j + z)\right\} - \log n_{cr}\right] \quad (8b)$$

For the general case, where the flight history is unknown, field calibration would specify the values for H_j and K_1 leaving as unknowns z, D_{cr}, n_{cr}, and $\bar{\alpha}$. It is then necessary to make measurements of H_{nj} as a function of n_j to determine $\bar{\alpha}$. If the block spectrum loading history develops flight-to-flight damage increments in accordance with the concept of the ground-air-ground cycle, then Eq. (8) can be simply evaluated with least-square plots. It is recommended that D_{cr} be determined from laboratory data. The least-square plots can then yield values of z and n_{cr}, the accuracy for which should improve as additional data are procured and analyzed.

The reliability of the over-all program is of course dependent upon the reliability of the established values of D_{cr} and their factors. Since flight-history measurements involve a reasonable period of time, it would be expedient to provide concurrent laboratory measurements to determine the sensitivity of D_{cr} to the various factors influencing it.

References

[1] Thompson, N. and Wadsworth, N. J., "Metal Fatigue," *Advances in Physics*, Vol. 7, 1958; also "Proceedings of the International Conference on Mechanisms of Fatigue in Crystalline Solids," *Acta Metallurgica*, Vol. 11, No. 7, July 1963.

[2] Wood, H. et al., "Systematic Microstructural Changes Pecu-

liar to Fatigue Deformation," *Acta Metallurgica*, Vol. 11, No. 7, July 1963, p. 643.

[3] Sinclair, G. M., *Proceedings of The American Society for Test Material*, Vol. 52, 1952, p. 743.

[4] "Symposium on the Role of Substructure in the Mechanical Behavior of Metals," ASD-TDR 63-324, April 1963, Air Systems Div., pp. 1–22.

[5] Zirinsky, S., Switsky, H., and Kenger, A., "Utilization of an Ultrasonic Fatigue Damage Indicator for Inspection and Design," *1966 Symposium for Reliability*, Nov. 1966, Los Angeles, Calif.

[6] Cory, G. et al., "Detection of Latent Fatigue Damage in Metals and Alloys," Contract NOw 59-1202-C, June 1960, Southwest Research Institute.

[7] Kunsenberger, F. et al., "Development of A Test Device for Study of Fatigue Damage," Contract NOw 61-0685-C, June 1962, Southwest Research Institute.

[8] Kusenberger, F. and Barton, "Experimental Substantiation of Fatigue Detection Capability," Contract N600 (19)-59307, June 1963, Southwest Research Institute.

[9] Kusenberger, F. et al., "Non-Destructive Evaluation of Metal Fatigue," AF 49(638)-1352, March 1965, AD61985, Southwest Research Institute.

[10] Kusenberger, F. et al., "Non-Destructive Evaluation of Metal Fatigue," AF 49(638)-1502, March 1966, Southwest Research Institute.

[11] Harting, D. "The *S/N* Fatigue Life Gage: A Direct Means for Measuring Cumulative Fatigue Damage," *Experimental Mechanics*, Feb. 1966.

[12] Brosius, H. et al., "Detection of Fatigue Damage with Rayleigh Waves," TR 60-307, Aug. 1960, Aeronautical Research Laboratory.

[13] Truell, R. et al., "The Use of Ultrasonic Methods to Determine Fatigue Effects in Metals," TR59-389, Nov. 1959, Wright Air Development Center.

[14] Rasmussen, J. G., "Prediction of Fatigue Failure Using Ultrasonic Surface Waves," Reprint 901, Krautkramer Ultrasonics Inc.

[15] Hardrath, H. F., "A Review of Fatigue Research in the United States," TM-X-56562, NASA.

JULY-AUG. 1968 J. AIRCRAFT VOL. 5, NO. 4

Automatic Flight Management of Future High-Performance Aircraft

DAVID M. PETRIE*
The Boeing Company, Seattle, Wash.

A developmental program to demonstrate the feasibility of automation as a means of improving the safety and profitability of commercial aircraft operations in the post-1975 era is underway. The integrated flight management system described herein employs a central computer onboard the aircraft to 1) control flight-path segments to precisely follow a flexibly programmed spacetime profile; 2) effect configuration control of the airplane and its principal subsystems; 3) automate the preflight check-list and equipment switching; 4) drive a multimode cathode ray tube display for monitoring equipment status and navigational situations; 5) effect automatic placarding for semimanual modes of flight operations; and 6) compute Mach number, effect c.g. control, store and display emergency operating procedures, and perform other similar functions that are amenable to centralized computing. Manual reversion for all automated functions is available. A similar increase in computerization of the air traffic control system is needed to best exploit the precise navigation and control capabilities of the automatic flight management (AFM) airplane in improving traffic flow and airport utilization. The need for planning is underscored by the many civilian and governmental organizations that desire to implement their related improvement programs in a coordinated way.

I. Introduction

THE role of the pilot in flight management of commercial aircraft has developed over the past four decades in quite logical fashion. As aircraft size, complexity, and speed have increased, we have found ways to display more information to the pilot, we have provided control surface power boost to augment his limited physical strength, and we have devised course-holding autopilots to free him from a routine task. The need to accelerate this evolution is underscored by a consideration of the following comparison in Table 1 between a typical commercial transport airplane of today and tomorrow's aircraft, such as the supersonic transport (SST).

Furthermore, runway acceptance rates and traffic handling procedures, as we know them today, exact an impressive toll on payload capacity and usable range, for aircraft like the SST, due to the large fuel reserves required. Precise navigation afforded by inertial navigation, digital data links between ground and airborne systems, and new autoland aids will avail a more orderly traffic management situation, relatively free of lengthy traffic holding patterns.

An analysis of the man/machine relationships which will be encountered in the operation of future aircraft has made it apparent that a modified philosophy of the role of the crew may be needed for operating large, fast aircraft, especially in the air-space environment circa 1980. This requirement is not generated specifically by supersonic speed, but by a com-

Presented as Paper 67–847 at the AIAA 4th Annual Meeting and Technical Display, Anaheim, Calif., October 23–27, 1967; submitted October 12, 1967; revision received March 21, 1968.

* Engineering Manager, Automatic Flight Management Research Project.